LIMNOLOGY and OCEANOGRAPHY

ASLO

*Limnol. Oceanogr.* 68, 2023, 2603–2616

doi: 10.1002/lno.12447

# Variability in lake bacterial growth and primary production under lake ice: Evidence from early winter to spring melt

**E. Henriikka Kivilä**,[1,2,3*] **Vilmantas Prėskienis**,[1,2,3] **Noémie Gaudreault**,[1,3] **Catherine Girard**,[1,2,3] **Milla Rautio**[1,2,3]

[1]Département des Sciences Fondamentales, Université du Québec à Chicoutimi, Chicoutimi, Québec, Canada
[2]Centre d'Études Nordiques (CEN), Université Laval, Québec, Québec, Canada
[3]Group for Interuniversity Research in Limnology and Aquatic Environment (GRIL), Montreal, Québec, Canada

## *Abstract*

Climate change is causing seasonally ice-covered lakes of the boreal region to undergo changes in their winter regime by altering patterns of precipitation and temperature, often reflected as reduced snow and ice cover duration. The duration, extent and quality of ice, and snow cover have a pivotal role for production and carbon cycling in lakes in winter, with potentially cascading effects for the following open water period. We investigated under-ice carbon cycling by assessing bacterial growth (including bacterial production, bacterial respiration, and bacterial growth efficiency) and primary production at five water depths during early winter, midwinter, late winter and melting season in a boreal lake, and report significantly different temporal patterns. Bacterial respiration was dominant in early and midwinter, whereas the late winter and melting season were dominated by bacterial production. Multiple linear regression models indicated that high early winter bacterial respiration was associated with senescing phytoplankton, whereas bacterial production was promoted by the onset of spring processes. Collectively, bacterial growth indices were inherently linked with bacterioplankton community composition and specific biomarker taxa. Primary production under ice increased in late winter when light-blocking snow cover melted, and primary production measured from the lake ice exceeded that of the water column at the melting season. Ice samples hosted diverse eukaryotic communities including photoautotrophs, suggesting that the habitat potential of the understudied lake ice and the role of ice for ecological processes at ice melt should be further explored.

With the majority of the world's lakes distributed north of the 40$^{th}$ latitude (Verpoorter et al. 2014), seasonally ice-covered lakes are a central component of the boreal landscape. Lake ice and potential snow cover on top form an efficient barrier reducing flows of heat, light, and material between the atmosphere and the lake water, resulting in much altered living conditions for the aquatic organisms (Cavaliere et al. 2021; Bramburger et al. 2022). In addition, the ice-covered period is threatened by climate change, resulting in, for example, reduced ice cover duration, changes in snow accumulation and ice formation (Sharma et al. 2021), altered timing of spring melt (Sadro et al. 2018), and associated physical and ecological changes in the water column (Hébert et al. 2021; Hrycik et al. 2022; Woolway et al. 2022).

Recent advances in winter limnology have greatly improved the understanding of physical winter processes (Cavaliere et al. 2021; Olsthoorn et al. 2022) and under-ice communities (Tran et al. 2018; McMeans et al. 2020; Shchapov et al. 2021). Yet, much remains unknown, especially considering links between the physical limnology and communities, resource availability, and food web functions, as well as their variability on spatial and temporal scales. While winter dormancy applies to various aquatic organisms, there is growing evidence of photosynthetic activity (Twiss 2012; Reinl et al. 2023) as well as rich and active microbial life and carbon processing under ice (Butler et al. 2019). This has implications for the proportion and extent to which carbon is mineralized to $CO_2$ or alternatively assimilated into biomass and potentially transferred into the food web.

*Correspondence: henriikka.kivila@uqac.ca



Additional Supporting Information may be found in the online version of this article.

**Author contribution statement:** E.H.K., M.R., V.P., and C.G. conceptualized the work, data were acquired, and analyzed by E.H.K., V.P., N.G., C.G., and M.R. E.H.K. drafted the manuscript. All authors contributed to and accepted the final version of the manuscript.

The importance of microbial processing for under-ice food webs is expected to increase as the classic phytoplankton-driven food web declines in low-light conditions (Jansen et al. 2021). In addition, the greenhouse gases accumulating during the ice-covered period (typically released at ice melt) contribute a significant portion of the annual greenhouse gas emissions from northern freshwaters (Denfeld et al. 2018), hence understanding microbial carbon processing under ice is fundamental for assessing annual carbon budgets of lakes and their links with the global carbon cycle (Karlsson et al. 2013). While sediment respiration accounts for majority of greenhouse gas production during winter (Denfeld et al. 2018), carbon processing by bacterioplankton under ice is less studied, and rates are rarely reported (but see Tulonen et al. 1994; Bižić-Ionescu et al. 2014; Kritzberg and Bååth 2022). During the open-water period, bacterioplankton growth patterns have been shown to be variable and often driven by dissolved organic matter (DOM) composition and allochthonous inputs (Ask et al. 2009; Berggren et al. 2010), as well as nutrients, particularly phosphorus (Smith and Prairie 2004; Vidal et al. 2011). Strong limnological gradients (including nutrients, carbon) can be present during the winter stratification of ice-covered lakes, and as bacterioplankton community structure also follows these biogeochemical gradients (Bertilsson et al. 2013), vertical and seasonal differences in bacterioplankton growth rates and carbon processing can be expected.

In this study, we aim to improve the understanding of microbial carbon processing under ice, by exploring bacterial growth, primary production, community assemblages and associated limnological and biogeochemical components in a boreal lake at four time periods and five depths across one winter. We further specify the most important environmental relationships and biomarkers for bacterial growth. In addition, we investigate the primary production potential and associated ice communities of the melting ice, to improve understanding of this poorly studied habitat, and elucidate the role of ice-derived material for the lake functioning at ice-off.

## Materials and methods

### Site description

The sampling campaign was conducted during the winter 2020–2021 on a medium-sized (83 ha) boreal Lake Simoncouche (48°25′N, 71°25′W; altitude 347 m) in Quebec, Canada. The lake is mesotrophic, dimictic, and shallow (mean depth 2.2 m, max. depth 8 m). Annual average water column concentration of dissolved organic carbon (DOC) is $5.3 \pm 0.8$ mg $L^{-1}$ and during the summer months the water temperatures exceed 20°C. The lake has typically been frozen between the end of November and the latter half of April or early May. In 2020, the lake froze over on 23 November and was ice free on 13 April 2021, with the maximum ice thickness (56 cm) occurring in early March. Typically, two to three phenologically different ice layers are present: at the bottom a layer of black ice (freezing from lake water), which is topped by white ice (freezing from snow and lake water) constituting most of the ice thickness. Toward the spring, a 3$^{rd}$ layer of slushy ice forms on the surface composed of white ice that is softened by sunlight and refreezes overnight in a daily cycle. The lake has one major inflow (contributing approximately 70% of incoming water) and one outflow at the opposite end of the lake. Mean water residence time is 50 d during the open water period, though variability is high (Vachon and del Giorgio 2014), and the winter residence time is similar (unpublished data).

### Sampling design

The sampling campaign extended over winter of 2020–2021, when sampling was conducted on four key time periods (sensu Jansen et al. 2021): early winter (14 December), mid-winter (23 February), late winter (23 March), and melting season (12 April). Water samples were retrieved from five specific depths (0 m, i.e., right below the ice, and from 1.5, 3, 4.5, and 7 m, calculated from the top of the ice) with a 2-liter Limnos (Limnos Ltd., Poland) water sampler for water chemistry, production measurements, and molecular analyses. One to three replicates were collected for different analyses and the sampling took place inside a pop-up tent minimizing light exposure. Physical water column properties (temperature, conductivity, dissolved oxygen [$O_2$] concentration) were profiled with a Ruskin RBR Concerto (RBR Ltd., Canada) multisonde. Snow and ice thickness were recorded. In addition, the lake was sampled during overturn in the fall (13 November 2020) and spring (26 April 2021) for the same variables as during winter, but from the mixed integrated water column. Ice samples were collected during the melting season, and subsampled to black ice, white ice, and slushy surface ice for molecular analyses. Bulk ice was collected for chlorophyll *a* (Chl *a*) and primary production measurements. Underwater light was monitored throughout the study with HOBO Pendant light sensors (Onset, USA) connected to a nearby mooring.

### Water chemistry, organic carbon components, and Chl *a*

From each date and depth, analyzed chemical components included pH, concentrations of total (nitrogen, TN; phosphorus, TP) and dissolved nutrients (soluble reactive phosphorus [SRP] and nitrate with negligible nitrite, referred to as $NO_3^-$), Chl *a*, dissolved organic carbon (DOC), and colored dissolved organic matter (CDOM) fractions. Water for dissolved components (SRP, $NO_3^-$, DOC, and CDOM) was filtered through precombusted GF/F filters (Whatman; nominal pore size 0.7 $\mu$m). DOC (two replicates) and nutrients were analyzed at the GRIL analytical laboratory of Université du Québec à Montréal (Montreal, Canada) following standard protocols. Measurements of pH (Fisher Scientific AR15) were conducted in the lab within a few hours after sampling.

For CDOM, spectral absorbance was measured to assess the absorption coefficients at 320 nm ($a_{320}$) and 440 nm ($a_{440}$), and specific ultraviolet absorbance at 254 nm (SUVA). The fluorescence spectra were recorded for a parallel factor (PARAFAC) model. Further details of the CDOM analyses and PARAFAC are provided in Supplementary Methods S1, Fig. S1, and Table S1. For Chl *a* analyses, 200–350 mL of lake water or melted ice was filtered through GF/F filters (three replicates per depth), extracted in ethanol and analyzed with a Cary Eclipse spectrofluorometer (Agilent Technologies) according to Nusch (1980). The extracts were scanned before and after acidification to subtract phaeopigments.

### Bacterial growth and primary production

Bacterial production was measured in-situ from five depths using tritiated leucine ($^3$H-leucine) and leucine-to-carbon conversion factor of 1.55 kg C mol Leu$^{-1}$. Samples with three replicates and two controls per depth were prepared by adding $^3$H-leucine (specific activity 160 Ci mmol$^{-1}$) to each vial to obtain a final concentration of 30 nM, at which bacteria were saturated (experimentally tested), and incubated in their respective depths in the lake. During the overturns, one sample set was produced from the mixed integrated water column (0–7 m). An incubation time of 1.5 h was defined from saturation curves produced preceding the in situ field experiment. Experiments were terminated by adding trichloroacetic acid (final concentration 5%) after which samples were stored in −20°C until centrifugation and radio assaying according to Smith and Azam (1992).

Bacterial respiration was measured as dissolved $O_2$ consumption using optical $O_2$ mini sensors (PSt3, PreSens, ± 1.4 $\mu$mol L$^{-1}$) and Fibox 4 oxygen meter (PreSens) (Warkentin et al. 2007). Within a few hours of sampling, three replicates of water from five specific depths during the ice-covered season, and from the integrated water column (0–7 m) during the spring overturn, were filtered through a 50-$\mu$m sieve to remove grazers and closed in 300-mL air-tight glass bottles without headspace. Incubations were carried out in an environmental chamber in darkness at 4°C. The samples, apart from the early winter samples, were placed in a water bath inside the climate chamber to further reduce temperature variability. The dissolved oxygen was measured 2–3 times a day, and the consumption was calculated as a linear regression slope between the stable starting concentration and the point where oxygen decrease became negligible (15–41 h).

Bacterial growth efficiency, reflecting proportion of bacterial production per unit of assimilated carbon, was calculated using the following equation and further expressed as percentage:

$$\mathrm{BGE} = \frac{\mathrm{BP}}{\mathrm{BP} + \mathrm{BR}}$$

where BGE stands for bacterial growth efficiency, BP stands for bacterial production, and BR stands for bacterial respiration.

Primary production was measured in situ with a $^{14}$C-$HCO_3$ method from five depths during late winter and melting season. These measures were not carried out during early and midwinter due to snow cover blocking the light under the ice. From each target depth three 20 mL replicates and two black controls were prepared (sample activity 0.2 $\mu$Ci mL$^{-1}$) and incubated for 1.5 h in their respective depth. In addition, samples from melted ice and integrated euphotic water column (down to 2.5 m in late winter and 3 m during melting season) or the whole water column (0–7 m; spring overturn) were incubated using a system generating a gradient of PAR introduced by Rae and Vincent (1998). In short, a box with five different light shades with two replicates each and two controls (0% light) were used to obtain photosynthesis vs. irradiance curves from complete darkness to full sunlight, to further determine the maximum primary production ($P_{max}$) via saturation curve according to Platt et al. (1980). All primary production samples were corrected for blanks and total activity of the samples.

### Molecular analyses

Molecular samples were collected as duplicates from three depths in the water column (0, 3, and 7 m) and from the 3 phenologically different ice layers in the melting season. Water samples were collected into low-density polyethylene Cubitainers (washed with 2%v/v Contrad 70 liquid detergent (DeconLabs) and 10%v/v ACS-grade HCl (Sigma-Aldrich), and rinsed with MilliQ and lake water), and ice was collected into sterile Whirl-Pak™ bags (Nasco). The water samples were filtered on the day of sampling, while the ice samples were melted at 4°C in the dark inside their collection bags and filtered once in liquid state within 3 days. The samples were filtered on to Sterivex™ (Whatman, pore size 0.22 $\mu$m) filters with a peristaltic pump (FH100M, Fisherbrand), filled with 2 mL of RNA later and stored at −80°C until processing. An average of 900 mL sample was passed on each filter; filtration was stopped based on coloration of the filters and reduced flow rate or running out of sample material.

DNA was extracted from Sterivex filters with the AllPrep DNA extraction kit (QIAGEN) following the method in Cruaud et al. (2017) and prepared into sequencing libraries targeting the V3–V4 regions of the 16S rRNA gene (primers 341F & 805R) (Herlemann et al. 2011), and the V4 region of the 18S gene (572F & 1009R) (Comeau et al. 2011). Sequencing was performed on an Illumina MiSeq and yielded 64,942 sequences for 16S and 28,116 for 18S. Reads were processed in R 4.3.1 (R Core Team 2023) with the DADA2 package v1.22.0 (Callahan et al. 2016). For full parameters used, see Supplementary Methods S2. Sequences were clustered into amplicon sequence variants (ASVs) and taxonomy was assigned with the

SILVA SSU v1.138.1 database for prokaryotes, and v.132 training set for eukaryotes (Quast et al. 2013; Yilmaz et al. 2014). Low abundance taxa (0.05%) as well as chloroplast-related sequences (in the 16S dataset) were removed. Diversity analyses were performed with the phyloseq v1.38.0 package (McMurdie and Holmes 2013).

### Statistical analyses

Statistical analyses were run in R (R Core Team 2023). Permutational ANOVA (PERMANOVA) with 999 permutations was used to define significance of differences between different depths and time periods for bacterial production, respiration and growth efficiency using the vegan v.2.6-4 package (Oksanen et al. 2020). To determine the factors driving the variability in bacterial production and respiration, environmental variables were tested in multiple linear regressions (MLR). The variables tested included temperature, conductivity, $O_2$ concentration, pH, TP, TN, SRP, $NO_3^-$, DOC, SUVA, $a_{440}$, $a_{320}$, and PARAFAC components C1–C4. Prior to the analysis sqrt-transformation (based on visual inspection) was applied to the response variables and to temperature, conductivity, $O_2$ concentration, TP, $NO_3^-$, SUVA, $a_{440}$, and C4. Non-transformed variables included in the models were pH, TN, SRP, and DOC; the final suite of variables was selected based on ecological significance and removal of autocorrelation (>0.9). The models were ranked according to their AICc scores using MuMIn v.1.47.1 package (Bartón 2022), and quality of the models was assessed with variable significance, diagnostic plots and heteroscedasticity of residuals. In addition, relative variable importance (RVI) was calculated from the 95% confidence interval set of the MLR models (9 models for production and 10 for respiration) to rank the relative importance of the variables considered by the MLR analysis (higher rank corresponding with higher importance) (Burnham and Anderson 2002).

A non-metric dimensional scaling (nMDS) was performed on the prokaryote community composition in water samples using the Bray–Curtis dissimilarity index (phyloseq package). Vectors representing bacterial production and respiration were further projected on the nMDS. As the nMDS suggested

**Table 1.** Physicochemical water column measurements at the four samplings (early, mid, and late winter, melting season) at five depths, and the integrated water column measurements for fall and spring overturns. Variables include temperature (Temp), specific conductivity (Cond), dissolved oxygen concentration ($O_2$ conc), total nitrogen (TN), total phosphorus (TP), soluble reactive phosphorus (SRP), nitrate ($NO_3^-$) and Chl *a*.

| Time Period | Depth (m) | pH | Temp (°C) | Cond ($\mu$S cm$^{-1}$) | $O_2$ conc (mg L$^{-1}$) | TN (mg L$^{-1}$) | TP ($\mu$g L$^{-1}$) | SRP ($\mu$g L$^{-1}$) | $NO_3^-$ ($\mu$g L$^{-1}$) | Chl *a* ($\mu$g L$^{-1}$) |
|---|---|---|---|---|---|---|---|---|---|---|
| Fall | 8.5 | 5.5 | 5.8 | 118.4 | 12.3 | 0.28 | 9.27 | 2.50 | 0.01 | 3.67 ± 0.03 |
| 13 Nov | | | | | | | | | | |
| Early | 0 | 7.5 | 1.28 | 110.0 | 13.1 | 0.66 | 8.3 | 3.2 | 0.04 | 2.3 ± 0.10 |
| 14 Dec | 1.5 | 7.6 | 2.92 | 118.4 | 12.2 | 0.25 | 6.8 | 6.6 | 0.02 | 1.9 ± 0.14 |
| | 3 | 7.4 | 3.73 | 120.8 | 10.2 | 0.30 | 7.9 | 4.3 | 0.02 | 1.82 ± 0.12 |
| | 4.5 | 7.1 | 4.00 | 155.3 | 6.6 | 0.42 | 8.5 | 5.3 | 0.01 | 1.16 ± 0.26 |
| | 7 | 7.3 | 4.50 | 340.5 | 5.4 | 0.41 | 13.5 | 8.3 | 0.04 | 0.94 ± 0.21 |
| Mid | 0 | 6.5 | 1.43 | 112.4 | 12.3 | 0.28 | 5.2 | 4.2 | 0.05 | 0.35 ± 0.02 |
| 23 Feb | 1.5 | 6.8 | 3.62 | 127.9 | 9.9 | 0.26 | 6.3 | 4.6 | 0.04 | 0.31 ± 0.03 |
| | 3 | 6.7 | 4.29 | 146.5 | 3.3 | 0.30 | 4.9 | 4.0 | 0.06 | 0.13 ± 0.01 |
| | 4.5 | 6.7 | 4.55 | 295.1 | 2.7 | 0.31 | 5.2 | 4.2 | 0.10 | 0.08 ± 0.01 |
| | 7 | 6.9 | 5.07 | 427.8 | 1.6 | 0.49 | 7.5 | 5.7 | 0.29 | 0.09 ± 0.00 |
| Late | 0 | 6.8 | 1.66 | 113.2 | 12.0 | 0.45 | 5.8 | 3.2 | 0.08 | 0.32 ± 0.03 |
| 23 Mar | 1.5 | 6.8 | 3.57 | 128.0 | 8.6 | 0.30 | 6.3 | 4.5 | 0.07 | 0.86 ± 0.17 |
| | 3 | 6.7 | 4.14 | 149.6 | 3.1 | 0.28 | 5.4 | 4.7 | 0.06 | 0.6 ± 0.03 |
| | 4.5 | 6.5 | 4.61 | 292.0 | 2.5 | 0.33 | 5.2 | 5.0 | 0.12 | 0.27 ± 0.00 |
| | 7 | 6.7 | 4.94 | 546.8 | 5.6 | 0.58 | 9.2 | 6.1 | 0.16 | 0.19 ± 0.17 |
| Melting | 0 | 6.3 | 4.75 | 32.3 | 11.8 | 0.17 | 5.5 | 1.9 | 0.05 | 1.05 ± 0.08 |
| 12 Apr | 1.5 | 6.7 | 4.63 | 139.2 | 11.4 | 0.25 | 5.9 | 3.4 | 0.06 | 1.76 ± 0.01 |
| | 3 | 6.6 | 4.00 | 178.5 | 3.8 | 0.24 | 5.7 | 4.5 | 0.07 | 1.55 ± 0.07 |
| | 4.5 | 6.7 | 4.63 | 357.4 | 2.5 | 0.34 | 12.1 | 5.9 | 0.13 | 0.96 ± 0.05 |
| | 7 | 6.8 | 4.87 | 643.6 | 2.6 | 0.53 | 6.8 | 6.5 | 0.10 | 0.67 ± 0.04 |
| Spring | 0–7 | 7.0 | 6.59 | 180.5 | 10.1 | 0.40 | 8.0 | 5.1 | 0.03 | 3.74 ± 0.12 |
| 26 Apr | | | | | | | | | | |

potential connections between the bacterioplankton community composition and growth patterns, samples were divided into three growth style groups based on their growth measurements: high bacterial production group (> 65 $\mu$g C $L^{-1}$ $d^{-1}$), high bacterial respiration group (> 65 $\mu$g C $L^{-1}$ $d^{-1}$) and a group with more balanced growth style (production and respiration < 65 $\mu$g C $L^{-1}$ $d^{-1}$). To identify biomarkers in these groups, a linear discriminant analysis effect size (LEfSe, Segata et al. 2011) was performed (microbiomeMarker 1.0.1 package, Cao et al. 2022) with significance level set to 0.5 and LDA cutoff to 4, and using one-against-all comparison between groups. Pairwise PERMANOVA (pairwiseAdonis package; Martinez Arbizu 2020) and betadisper comparisons (vegan package) were used to determine if the groups differed in community composition.

## Results

### Physicochemical and carbon properties

Temporal and vertical gradients were evident in the limnological data, displaying typical winter stratification patterns (Table 1). Temperature was inversely stratified, and the thermocline was close to the surface (above 1.5 m) throughout the first three periods, but not present at the melting season. Solute (conductivity) and $O_2$ concentrations remained stratified for the whole study period, with higher conductivity and lower oxygen concentration at the bottom. As an exception, bottom water was oxygen-rich during late winter, when a lateral flow from the littoral was located at the lake bottom based on the density gradient of the water column (unpublished data). In early winter pH was slightly alkaline while otherwise slightly acidic. During the melting season pH was noticeably lower at 0 m, this sample was characterized by remarkably low conductivity and low nutrient concentrations, particularly SRP (Table 1). TP levels in early winter were elevated compared to other time periods. Chl *a* was generally low under ice and highest in early winter. The highest values were close to the surface in early and midwinter, whereas a clear Chl *a* maximum during late winter and melting season was at 1.5 m. Chl *a* was similar during fall and spring overturns, and higher than under ice.

The PARAFAC analysis identified four carbon components (C1–C4; Supplementary Table S1). Components C1–C3 represented humic-like matter with likely terrestrial origin (C2 potentially microbially reworked terrestrial material) and were highly correlated. C4 had a tyrosine-like signature

**Table 2.** Concentration and properties of DOC, including spectral indices (absorption at 320 and 440 nm, specific UV-absorbance: SUVA), fluorescent dissolved organic matter (FDOM) and the PARAFAC components C1–C4 under the ice. Fall and spring overturn data are for the integrated water column.

| Time period | Depth (m) | DOC (mg $L^{-1}$) | SUVA | $a_{320}$ ($m^{-1}$) | $a_{440}$ ($m^{-1}$) | C1 (RU) | C2 (RU) | C3 (RU) | C4 (RU) | FDOM (RU) |
|---|---|---|---|---|---|---|---|---|---|---|
| Fall | 0–6 | 6.55 ± 0.21 | 3.3 | 17.63 | 2.10 | 1.06 | 1.16 | 0.43 | 0.25 | 2.9 |
| Early | 0 | 6.4 ± 0.14 | 3.0 | 16.37 | 1.98 | 1.01 | 1.06 | 0.37 | 0.36 | 2.80 |
| | 1.5 | 6.2 ± 0.00 | 3.2 | 16.24 | 2.30 | 0.98 | 1.07 | 0.37 | 0.49 | 2.91 |
| | 3 | 6.15 ± 0.07 | 3.3 | 17.04 | 2.39 | 1.04 | 1.13 | 0.41 | 0.24 | 2.82 |
| | 4.5 | 6.2 ± 0.14 | 3.1 | 16.22 | 2.37 | 1.15 | 1.20 | 0.43 | 0.54 | 3.32 |
| | 7 | 7.35 ± 0.49 | 3.2 | 20.87 | 2.72 | 1.62 | 1.51 | 0.65 | 0.72 | 4.50 |
| Mid | 0 | 6.15 ± 0.07 | 3.0 | 15.41 | 1.91 | 1.13 | 1.26 | 0.46 | 0.26 | 3.12 |
| | 1.5 | 5.65 ± 0.21 | 3.3 | 15.66 | 1.80 | 1.22 | 1.31 | 0.49 | 0.23 | 3.26 |
| | 3 | 5.7 ± 0.00 | 3.3 | 15.59 | 1.78 | 1.31 | 1.36 | 0.52 | 0.21 | 3.40 |
| | 4.5 | 6.2 ± 0.14 | 3.1 | 16.65 | 1.81 | 1.37 | 1.40 | 0.56 | 0.23 | 3.56 |
| | 7 | 7.5 ± 0.00 | 3.5 | 24.22 | 3.04 | 1.86 | 1.74 | 0.82 | 0.17 | 4.60 |
| Late | 0 | 6.5 ± 0.14 | 3.0 | 16.11 | 1.93 | 1.00 | 1.15 | 0.36 | 0.33 | 2.83 |
| | 1.5 | 6.1 ± 0.42 | 3.2 | 15.86 | 1.97 | 1.01 | 1.13 | 0.39 | 0.22 | 2.75 |
| | 3 | 5.9 ± 0.00 | 3.3 | 15.86 | 1.97 | 1.08 | 1.15 | 0.43 | 0.19 | 2.85 |
| | 4.5 | 6.25 ± 0.07 | 3.2 | 17.28 | 2.04 | 1.24 | 1.25 | 0.51 | 0.19 | 3.18 |
| | 7 | 7.85 ± 0.21 | 3.9 | 31.45 | 5.13 | 1.54 | 1.42 | 0.68 | 0.17 | 3.81 |
| Melting | 0 | 3.25 ± 1.10 | 3.7 | 11.02 | 1.45 | 0.56 | 0.48 | 0.21 | 0.09 | 1.33 |
| | 1.5 | 5.5 ± 0.14 | 3.3 | 15.53 | 1.97 | 0.89 | 0.90 | 0.33 | 0.15 | 2.27 |
| | 3 | 5.7 ± 0.14 | 3.2 | 15.53 | 1.75 | 0.98 | 1.00 | 0.39 | 0.15 | 2.52 |
| | 4.5 | 6.5 ± 0.14 | 3.2 | 18.64 | 2.26 | 1.14 | 1.12 | 0.48 | 0.14 | 2.88 |
| | 7 | 7.05 ± 0.07 | 3.3 | 22.02 | 2.81 | 1.30 | 1.20 | 0.57 | 0.14 | 3.21 |
| Spring | 0–7 | 5.05 ± 0.07 | 3.42 | 14.86 | 1.97 | 0.66 | 0.69 | 0.24 | 0.13 | 1.72 |

and was interpreted as a protein-like autochthonous component, which since peaking in the early winter, is likely reflecting DOM originating from senescing phytoplankton in our study. Total fluorescent organic matter (FDOM) indicates the sum of C1–C4. For DOC and all carbon indices highest values occurred at the lake bottom throughout the winter

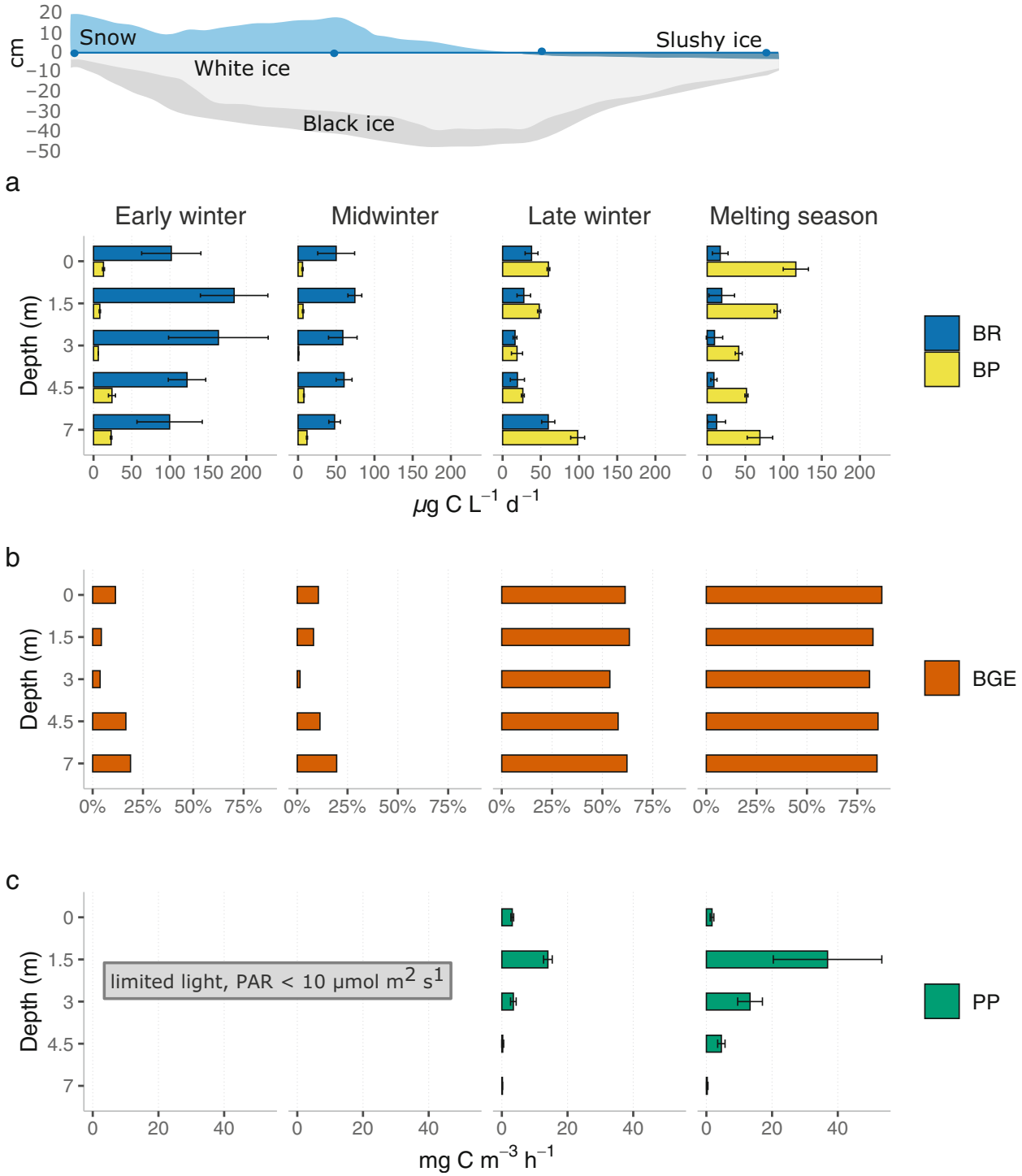


**Fig. 1.** Results from different time periods at specific depths for (**a**) bacterial respiration (BR) and bacterial production (BP), (**b**) bacterial growth efficiency (BGE) and c) primary production (PP). Mean and standard deviation among replicates are given. Snow and ice layer thickness across the study period are presented on top, the dots on the vertical line of the ice panel represent the sampling moments.

(Table 2.). In the early winter $a_{440}$ and C4 displayed elevated values. During the melting season all carbon indices were diluted at 0 m. DOC was elevated during the fall overturn, in respect to the under-ice average ($6.21 \pm 0.64$ mg $L^{-1}$) and the spring overturn.

### Bacterial growth patterns

Across the studied winter, bacterial production varied between 0.83 and 116 $\mu$g C $L^{-1}$ $d^{-1}$, with lowest values occurring during midwinter and highest during the melting season (Fig. 1.). During the preceding open water period bacterial production was higher (fall overturn, $40.8 \pm 1.9$ $\mu$g C $L^{-1}$ $d^{-1}$) than after formation of ice in early winter (< 25 $\mu$g C $L^{-1}$ $d^{-1}$), whereas after the ice-off it was reduced from high under-ice values (> 40 $\mu$g C $L^{-1}$ $d^{-1}$) to $14.92 \pm 2.0$ $\mu$g C $L^{-1}$ $d^{-1}$ during spring overturn. Bacterial production was most active at greater depths from early to late winter, but during the melting season the highest production occurred right under the ice. The lowest production occurred consistently in the intermediate depths. Bacterial respiration varied from negligible to 234 $\mu$g C $L^{-1}$ $d^{-1}$ under the ice cover, dominating the carbon metabolism from early to late winter. It was highest during early winter (> 100 $\mu$g C $L^{-1}$ $d^{-1}$ per depth) and lowest during melting season (< 20 $\mu$g C $L^{-1}$ $d^{-1}$ per depth). Bacterial growth efficiency ranged from 1.4% to 87% being lower (< 20%) during early and midwinter but increased considerably (> 50%) toward late winter and further (> 80%) during the melting season. During spring overturn respiration increased ($348 \pm 12$ $\mu$g C $L^{-1}$ $d^{-1}$) and growth efficiency reduced (4%) remarkably compared to previous under-ice conditions. PERMANOVA revealed that there were significant differences between the time periods ($R^2 = 0.70$, $p = 0.001$). The time period was significant ($p = 0.001$) to all growth variables explaining majority of the variance (production: $R^2 = 0.64$, respiration: $R^2 = 0.72$, growth efficiency: $R^2 = 0.98$). Depth was significant only to growth efficiency ($R^2 = 0.003$, $p = 0.003$), whereas the interaction term (Period : Depth) was significant for production ($R^2 = 0.09$, $p = 0.002$) and growth efficiency ($R^2 = 0.04$, $p = 0.012$).

### Environmental relationships with bacterial production and respiration

Several significant relationships with bacterial production and respiration were identified through MLR and RVI analyses. For production, the best MLR model ($R^2_{adj} = 0.54$, $p = 0.003$) included variables that typically respond strongly to spring onset; temperature, $O_2$ concentration, pH (inverse relationship), and TN. Variability in respiration was best explained by the MLR model ($R^2_{adj} = 0.76$, $p < 0.001$) that included pH, SUVA (inverse relationship), TP and C4 that reflect the early winter conditions with senescing algae. The variables identified by the RVI analysis displayed over four times more importance than any other tested variable for production and over twice for respiration (Supplementary

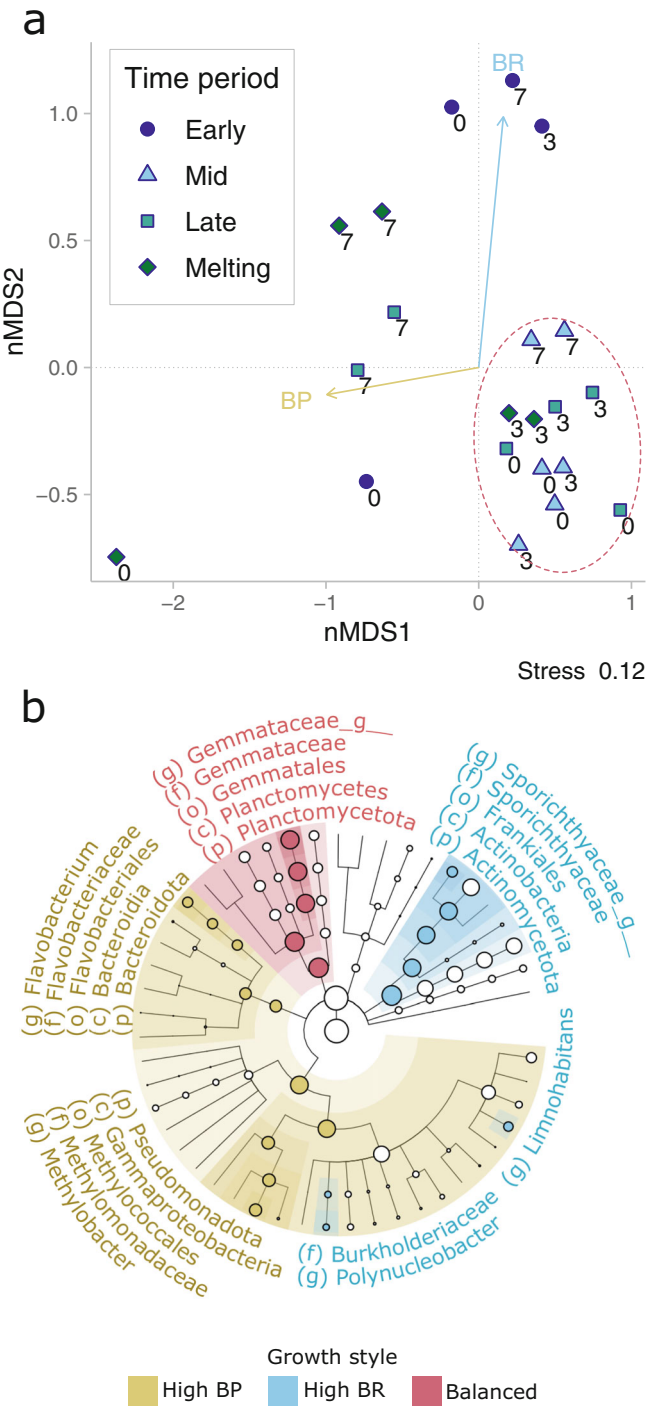


**Fig. 2.** (**a**) An nMDS plot of bacterioplankton community composition from a Bray–Curtis dissimilarity matrix, presenting samples from 0, 3, and 7 m depths at four winter time periods. Vectors of bacterial production (BP) and respiration (BR) are presented on top to show relationships between microbial community and bacterial growth styles. The dashed red oval marks the samples corresponding with the balanced growth style. (**b**) Phylogeny of significant bacterioplankton biomarkers associated with the three observed growth styles (high production [BP], high respiration [BR], balanced). The significant biomarkers (filled dots) are named outwards from the center, following phylogenetic ranks: phylum (p), class (c), order (o), family (f), genus (g).

Fig. S2). Correlations between individual variables are presented in Supplementary Table S2.

### Association of bacterial growth with bacterioplankton community composition

Molecular analyses revealed that the bacterioplankton community composition (Supplementary Fig. S3) was correlated with heterotrophic bacterial growth patterns. In the community composition nMDS (Fig. 2a), bacterial production aligned with nMDS1, while bacterial respiration correlated with nMDS2. A group of samples in the lower right corner of the nMDS plot corresponded with the predefined balanced growth style group used in the LEfSe analysis, which revealed 23 significant biomarkers for the growth style groups: high production, high respiration and balanced (10, 8, and 5 biomarkers, respectively; Fig. 2b). The balanced group was characterized by Planctomycetota, especially the order of Gemmatales, whereas high production was associated taxa in two phylums: *Flavobacterium* (Bacteroidota) and *Methylobacter* (Pseudomonadota). High respiration was featured by *Sporichthyaceae* (Actinobacteria) in addition to three specific biomarkers within Gammaproteobacteria: *Limnohabitans* and *Polynucleobacter* genera, and the Burkholderiaceae. Bacterioplankton assemblages grouped according to growth style were significantly different and the grouping explained 40.2% of assemblage composition variance (PERMANOVA, $p = 0.001$). Dispersion within the groups was homogenous (betadisper, $p > 0.05$).

### Primary production in water and ice

After snow melted and light returned under the ice in March (Supplementary Fig. S4), primary production (in situ) under the ice varied from 0.18 to 36.9 mg C $m^{-3}$ $h^{-1}$. An increasing trend from late winter to melting season was observed, with highest production occurring consistently at 1.5 m depth (Fig. 1.). In agreement, $P_{max}$ from the water presented an increasing trend from late winter (36 mg C $m^{-3}$ $h^{-1}$) to melting season (151 mg C $m^{-3}$ $h^{-1}$) and further into the spring overturn (817 mg C $m^{-3}$ $h^{-1}$). The melting ice had higher $P_{max}$ values (208 mg C $m^{-3}$ $h^{-1}$) than the underlying water column, which was further corroborated by a similar, statistically significant (Welch's *t*-test, $p = 0.02$) pattern in Chl *a* (ice: $1.56 \pm 0.17$ $\mu g$ $L^{-1}$, water:

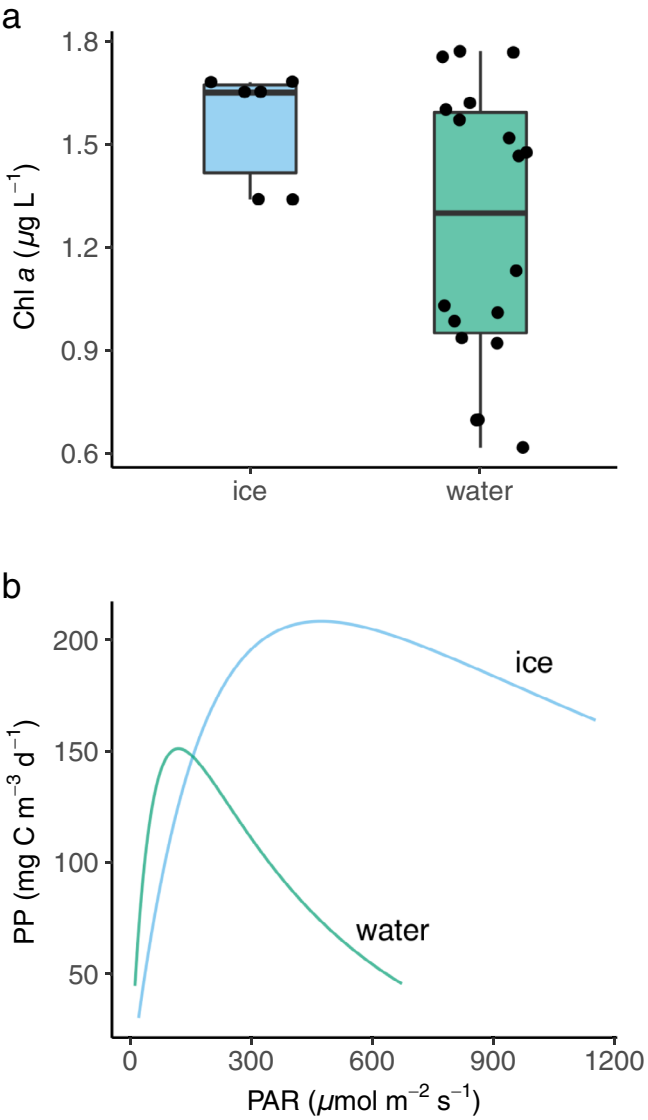


**Fig. 3.** Comparison of algal community responses between ice and water during the melting season for (**a**) Chl *a* concentration (significant difference) and (**b**) photosynthesis–irradiance curves. PP = primary production, PAR = photosynthetically active radiation.

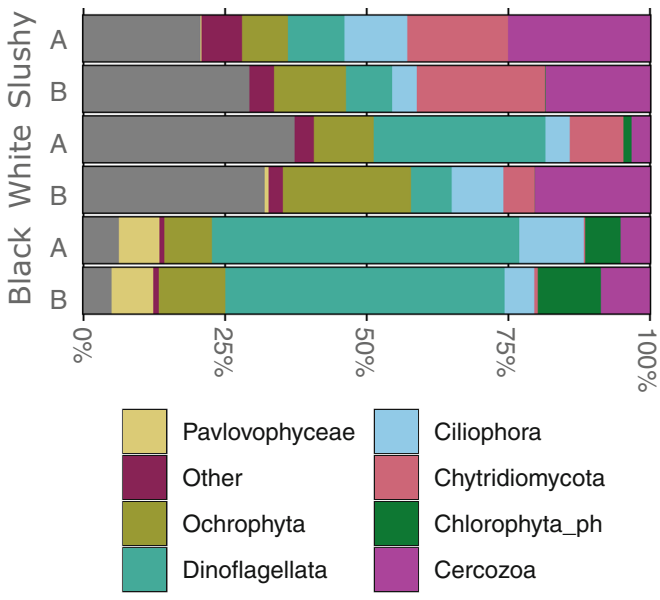


**Fig. 4.** Relative abundance of microbial eukaryotes (18S) in the melting ice. The gray bar represents unidentified sequences. Two replicates (A, B) were analyzed from each phenologically different ice layer (black, white, and slushy).

$1.26 \pm 0.40\ \mu g\ L^{-1}$) (Fig. 3a). Furthermore, the photosynthesis–irradiance curves showed not only higher $P_{max}$ but also lower photoinhibition for the ice community (Fig. 3b).

### Microbial eukaryote community composition in the ice

A diverse community of autotrophic and mixotrophic protists was observed in the melting ice (Fig. 4). Dinoflagellates were the most abundant group particularly in black ice, followed by ochrophytes (including diatoms and chrysophytes), haptophytes, chlorophytes, and ciliates. Phenologically different ice layers differed in their community composition, with higher diversity toward the bottom (Chao1: 85.5, 100.5, 154.5, for slushy, white, and black ice, respectively), and more even communities in the upper parts (Shannon: 3.43, 3.54, and 3.24, for slushy, white, and black ice, respectively). The thickest ice layer at the time was the white ice.

## Discussion

### Development of bacterial growth under ice

Overall, the observed level of bacterial production, respiration, and growth efficiency in this study indicate active, under-ice carbon processing, both via mineralizing and converting organic carbon to biomass. Measured values of bacterial respiration and production in the lake represent typical values for the boreal region (Berggren et al. 2009, 2010), but are higher than most reported winter values (Tulonen et al. 1994; Bastviken et al. 2003; Grosbois et al. 2020).

The total processed bacterial carbon (sum of respiration and production at all five depths) was nearly twofold greater in early winter, compared to the other time periods, and heavily relied on respiration. Brentrup et al. (2021) demonstrated a similar pattern with high lake respiration in early winter in Lake Sunapee, New Hampshire, USA. Midwinter revealed reduced rates of microbial carbon processing, which may be associated with reduced availability of decaying algal carbon, lower temperatures, and lack of light and water flow, representing a deep winter slow down caused by limited resources (Bertilsson et al. 2013; Jansen et al. 2021). Bacterioplankton can swiftly respond to changes in environmental drivers due to rapid biomass turnover, and while bacterial production is often limited under ice compared to open water period (Bertilsson et al. 2013), our results suggest that the late winter and melting season can provide an environment favorable for bacterial production.

The increasing bacterial growth efficiency from early to late winter was in a typical range for boreal lakes during the open water period, however, compared to previous spring measurements, the melting season values were high (Berggren et al. 2010). As the respiratory quotient in the conversion of respired oxygen to carbon was assumed 1, it is possible that our bacterial respiration values represent an underestimation, particularly applying to the late winter and melting season samples, where photodegradation processes may have altered the composition of carbon substrate pool (Allesson et al. 2016), leading to an overestimation of bacterial growth efficiency. Similarly, leucine-to-carbon conversion factors can vary seasonally but have been shown to be close to the here used theoretical value of 1.55 kg C mol $Leu^{-1}$ in winter (Calvo-Díaz and Morán 2009). We consider the conversion factors, despite causing some inaccuracy in the calculations, to have a minor effect on the growth efficiency trends depicted by our data. The prevailing trend in bacterial growth efficiency suggests that during the early and midwinter much of the microbially processed carbon is mineralized to $CO_2$, whereas during the late winter and melting season a greater proportion of carbon is available to fuel the aquatic food web as biomass.

### Controls of bacterial growth

Requirements for growth of heterotrophic bacteria include temperature, organic carbon and nutrients; however, to date it remains poorly understood to which extent each prerequisite dominates in under-ice conditions. According to the MLR models, bacterial production was promoted by temperature, TN, $O_2$ and lower pH, suggesting a clear connection with the spring runoff and late winter physicochemical processes (*see* Jansen et al. 2021). For most of the winter, bacterial production was highest at the bottom, where nutrient rich and warmer conditions favor microbial activity (Bertilsson et al. 2013). Temperature has previously been observed to have a stronger relationship with bacterial production during winter than summer (Tulonen et al. 1994), and drainage from forested catchments has boosted bacterial production and growth efficiency (Berggren et al. 2009). An additional important aspect of spring processes is the increasing amount of light, which can restructure the DOM pool through photochemical transformation, and thus boost bacterial production by providing bioavailable nutrients and carbon fractions (Vähätalo et al. 2003; Mazoyer et al. 2022), as well as boost primary production, which has also been linked to higher bacterial production (Straškrábová et al. 2005; Bižić-Ionescu et al. 2014).

Bacterial respiration showed a significant positive relationship with pH and a protein-like fluorophore C4, both with above 50% importance, while TP and SUVA were less important but significant variables. High occurrence of TP and C4, and low SUVA, during early winter indicate more abundant autochthonous low-molecular-weight organic material. Hence, our results suggest that the carbon composition and availability of senescing algae are major factors for respiration under the ice cover, which is in agreement with previous studies (Bižić-Ionescu et al. 2014; Reinl et al. 2023). Accordingly, Guillemette et al. (2016) stated that autochthonous carbon is preferentially selected for respiration, whereas terrestrial substrates are more allocated for production. The role of pH was important for both bacterial production and respiration and has been previously noted as a major regulator of bacterial carbon processing (Tank et al. 2009).

### Molecular biomarkers associated with bacterial growth

Bacterioplankton community composition showed clear connections with the bacterial growth patterns (Fig. 2), and significant biomarker taxa were identified for all three growth styles (high production, high respiration, and balanced). The balanced group, prevailing mostly during mid- and late winter, was characterized by Planctomycetes, which have been previously found enriched under ice (Butler et al. 2019), and especially the family Gemmataceae. Only few studies on Gemmataceae have been published to date, but they are ubiquitous and include cold-adapted, psychrotolerant taxa (Kulichevskaya et al. 2020). Some Gemmataceae have a nutritional preference for polysaccharides, such as xylan and pectin (Ivanova et al. 2021), suggesting a connection with terrestrial organic matter. However, abundance of Gemmataceae has been found to correlate with both allochthonous and autochthonous DOM components, with some phylotypes expressing metabolic preference for tryptophan-like DOM (Zhang et al. 2019).

Significant biomarkers with high respiration targeted the Actinomycetota, especially the family Sporichthyaceae, as well as specific (*Polynucleobacter*, *Limnohabitans*, Bulkholderiaceae) biomarkers within Gammaproteobacteria. *Polynycleobacter* and *Limnohabitans* have been described to have substrate-driven, plastic organic matter utilization strategies with preference on algal-derived carbon, and tendency to respire it (Horňák et al. 2017). Furthermore, Ávila et al. (2019) reported that both *Limnohabitans* and Sporichthyaceae demonstrate a preference for low-molecular-weight carbon (i.e., algal sources). While *Polynucleobacter* and Sporichthyaceae have wider tolerance for pH, *Limnohabitans* are neutro-alkaliphiles (Šimek et al. 2010), linking the molecular biomarkers and environmental controls of bacterial respiration (pH and carbon sources C4, SUVA, TP) together, and suggesting that the early winter conditions support bacterioplankton favoring high respiration as their growth style.

Significant biomarkers for high production included two major groups: genera *Methylobacter* in Pseudomonadota and *Flavobacterium* in Bacteroidota, which are well in line with the existing literature. Methanotrophic *Methylobacter* taxa are common in stratified lakes; they thrive in both oxygenated and anoxic conditions (van Grinsven et al. 2020). Methanotrophs in general have been formerly shown to contribute a significant portion of bacterial production in boreal lakes, and even more so during winter time (Bastviken et al. 2003; Kankaala et al. 2006). Flavobacteria have been shown to increase activity with increasing phytoplankton concentration, and be able to efficiently utilize freshly produced algal exudates (Sarmento et al. 2016), suggesting a link with the increasing primary production initiated by light availability. On the other hand, it has been suggested that Flavobacteria also have a preference for high-molecular-weight carbon and terrestrial, humic DOM (Amaral et al. 2016). Based on mesocosm experiments, Ávila et al. (2019) suggested that specialized groups of bacterioplankton shape the DOM pool via resource partitioning, preferring either low (Sporichthyaceae) or high (Gammaproteobacteria–Flavobacteria) molecular weight carbon. The see-saw pattern between the high bacterial respiration with algal DOM and high bacterial production with terrestrial DOM observed in our data, thus corresponds with previous findings considering both bacterioplankton community composition (Ávila et al. 2019) and tendency to either assimilate or mineralize certain carbon sources (Guillemette et al. 2016).

### Primary production in and under the ice

Various studies have shown the primary production potential under lake ice (e.g., Bramburger et al. 2022) and the under-ice bloom may be even more intense than the spring/summer bloom following ice-out, particularly in polar (Imbeau et al. 2021), but also boreal and temperate lakes (Twiss 2012; Salmi and Salonen 2016). In this study under-ice primary production never reached the open water spring bloom levels, suggesting that the ice-derived light limitation can still effectively suppress primary production in boreal systems. The peak in situ primary production under ice (at 1.5 m) reached only 39% efficiency in late winter and 24% efficiency during the melting season, as derived from the $P_{max}$ for the euphotic zone. The clear vertical preference of 1.5 m is presumably caused by the optimal combination of light, temperature, and nutrient availability: light availability is highly suppressed in the lower water column, whereas the conditions right below the ice are cold and diluted in nutrients. Too intensive solar or UV irradiation right under the ice may also inhibit primary production, as the water column communities were adapted to low-light conditions. Solar radiation, controlled especially by the snow cover, is a major controller of under-ice phytoplankton (Song et al. 2019).

Unexpectedly, the highest $P_{max}$ during the ice-covered season was recorded from the melting ice, being comparable with measurements from arctic sea ice (Leu et al. 2015). The result was further supported by higher Chl *a* levels in ice compared to the underlying water, and a similar Chl *a* pattern has been previously reported from Lake Simoncouche (Imbeau et al. 2021). Traditionally, lake ice has not been deemed as a potential habitat for any relevant production, due to its denser structure in comparison to sea ice. However, during the melting season ice disintegrates through extensive vertical cracking: this allows infiltration of lake water into large areas of the ice cover, creating a poorly explored lake ice habitat with many shared characteristics with sea ice.

### The ice habitat

The melting ice hosted a diverse community of photosynthetic eukaryotes: most abundant, particularly in the black ice layer, were dinoflagellates, dominated by *Gymnodinium*. These photoautotrophic, small flagellates are significant components of under-ice blooms in Lake Baikal, and have also been observed in the porous ice (Obolkin et al. 2019). Ochrophytes, another large component of the ice community, composed

nearly entirely of chrysophytes with dominance of genera *Hydrurus* and *Chrysocapsa*. Photoautotrophic *Hydrurus* species have been observed from polar and glacial snow habitats (Winkel et al. 2022) and cold streams, where they have dominated the spring Chl *a* peak (Rott et al. 2006). The majority of primary production in ice was likely carried out by eukaryotic organisms, but a small amount of cyanobacteria was also detected in the slushy ice with 16S sequencing (Supplementary Fig. S5). Sequencing data from lake ice are sparse, and while no conclusion about the viability of the organisms based on sole presence of DNA can be drawn, viable phytoplankton have still been observed in river ice in Quebec (Frenette et al. 2008), and in the ice cover of Lake Erie (Twiss 2012), where they have also been suggested to be preferentially incorporated into the ice. The infiltrated ice can serve as a predation-free refuge for flagellates originating from the water column or the ice itself, as Imbeau et al. (2021) has previously reported a consistent presence of phytoplankton cells in Lake Simoncouche ice throughout a winter season.

Non-photosynthesizing protists in the ice included diverse heterotrophs, such as cercozoans, comprising of predatory or parasitic ameboids and flagellates (Cavalier-Smith and Chao 2003), and Chytridiomycota, which are well-known parasites for freshwater algae and capable of altering food-web processes (Sime-Ngando 2012). These two phyla were more common in the upper parts of the ice and might thus be atmospherically deposited. Regardless, our data suggests that freshwater ice incorporates a suite of diverse biotic components from different sources, thus manifesting habitat complexity and supporting the view that lake ice acts like a "second bottom" (Hampton et al. 2015). A suite of microorganisms with diverse life strategies is released into the lake from melting ice, which may have cascading effects to the aquatic life during the spring bloom.

## Conclusions

In this study we presented strong, temporal patterns of bacterioplankton production, respiration and growth efficiency under ice. Early winter was dominated by respiration, favored by phytoplankton legacy effects from the previous open water period, whereas the onset of spring processes led to high dominance of biomass production during the late winter and melting season, as well as increased primary production. These patterns were concomitant with changes in bacterioplankton community composition and bioindicator taxa associated with different growth styles, suggesting that the under-ice bacterioplankton carbon processing is dependent on both environmental factors and community composition. Our results suggest that, during the melting season, microbial life under ice is remarkably active on an annual scale, featured with high growth efficiency. In addition, we report high primary production in the melting ice. These findings highlight the importance of further studies on the melting season dynamics and lake ice ecology, as these conditions set the starting point for the following open water period.

### Data availability statement

The data that support the findings of this study are openly available at Borealis, the Canadian Dataverse Repository (https://borealisdata.ca), at https://doi.org/10.5683/SP3/AWHLCK. The sequencing data are available at NCBI SRA under BioProject ID PRJNA1011868.

## References

Allesson, L., L. Ström, and M. Berggren. 2016. Impact of photochemical processing of DOC on the bacterioplankton respiratory quotient in aquatic ecosystems. Geophys. Res. Lett. **43**: 7538–7545. doi:10.1002/2016GL069621

Amaral, V., D. Graeber, D. Calliari, and C. Alonso. 2016. Strong linkages between DOM optical properties and main clades of aquatic bacteria: Bacterioplankton links to DOM properties. Limnol. Oceanogr. **61**: 906–918. doi:10.1002/lno.10258

Ask, J., J. Karlsson, L. Persson, P. Ask, P. Byström, and M. Jansson. 2009. Terrestrial organic matter and light penetration: Effects on bacterial and primary production in lakes. Limnol. Oceanogr. **54**: 2034–2040. doi:10.4319/lo.2009.54.6.2034

Ávila, M. P., and others. 2019. Linking shifts in bacterial community with changes in dissolved organic matter pool in a tropical lake. Sci. Total Environ. **672**: 990–1003. doi:10.1016/j.scitotenv.2019.04.033

Bartón, K. 2022. MuMIn: Multi-model inference. R package version 1.47.1. Available from https://CRAN.R-project.org/package=MuMIn.

Bastviken, D., J. Ejlertsson, I. Sundh, and L. Tranvik. 2003. Methane as a source of carbon and energy for lake pelagic food webs. Ecology **84**: 969–981 doi:10.1890/0012-9658(2003)084[0969:MAASOC]2.0.CO;2.

Berggren, M., H. Laudon, and M. Jansson. 2009. Hydrological control of organic carbon support for bacterial growth in boreal headwater streams. Microb. Ecol. **57**: 170–178. doi:10.1007/s00248-008-9423-6

Berggren, M., H. Laudon, M. Haei, L. Ström, and M. Jansson. 2010. Efficient aquatic bacterial metabolism of dissolved low-molecular-weight compounds from terrestrial sources. ISME J. **4**: 408–416. doi:10.1038/ismej.2009.120

Bertilsson, S., and others. 2013. The under-ice microbiome of seasonally frozen lakes. Limnol. Oceanogr. **58**: 1998–2012. doi:10.4319/lo.2013.58.6.1998

Bižić-Ionescu, M., R. Amann, and H.-P. Grossart. 2014. Massive regime shifts and high activity of heterotrophic bacteria in an ice-covered lake. PloS One **9**: e113611. doi:10.1371/journal.pone.0113611

Bramburger, A. J., T. Ozersky, G. M. Silsbe, C. J. Crawford, L. G. Olmanson, and K. Shchapov. 2022. The not-

so-dead of winter: Underwater light climate and primary productivity under snow and ice cover in inland lakes. Inland Waters **10**: 10–12. doi:10.1080/20442041.2022.2102870

Brentrup, J. A., D. C. Richardson, C. C. Carey, N. K. Ward, D. A. Bruesewitz, and K. C. Weathers. 2021. Under-ice respiration rates shift the annual carbon cycle in the mixed layer of an oligotrophic lake from autotrophy to heterotrophy. Inland Waters **11**: 114–123. doi:10.1080/20442041.2020.1805261

Burnham, K. P., and D. R. Anderson. 2002. Model selection and multimodel interference: A practical information-theoretic approach. Springer.

Butler, T. M., A.-C. Wilhelm, A. C. Dwyer, P. N. Webb, A. L. Baldwin, and S. M. Techtmann. 2019. Microbial community dynamics during lake ice freezing. Sci. Rep. **9**: 6231. doi:10.1038/s41598-019-42609-9

Callahan, B. J., P. J. McMurdie, M. J. Rosen, A. W. Han, A. J. A. Johnson, and S. P. Holmes. 2016. DADA2: High-resolution sample inference from Illumina amplicon data. Nat. Methods **13**: 581–583. doi:10.1038/nmeth.3869

Calvo-Díaz, A., and X. A. G. Morán. 2009. Empirical leucine-to-carbon conversion factors for estimating heterotrophic bacterial production: Seasonality and predictability in a temperate coastal ecosystem. Appl. Environ. Microbiol. **75**: 3216–3221. doi:10.1128/AEM.01570-08

Cao, Y., Q. Dong, D. Wang, P. Zhang, Y. Liu, and C. Niu. 2022. microbiomeMarker: An R/Bioconductor package for microbiome marker identification and visualization. Bioinformatics **38**: 4027–4029. doi:10.1093/bioinformatics/btac438

Cavaliere, E., and others. 2021. The Lake ice continuum concept: Influence of winter conditions on energy and ecosystem dynamics. J. Geophys. Res. Biogeo. **126**: e2020JG006165. doi:10.1029/2020JG006165

Cavalier-Smith, T., and E. E.-Y. Chao. 2003. Phylogeny and classification of phylum Cercozoa (protozoa). Protist **154**: 341–358. doi:10.1078/143446103322454112

Comeau, A. M., W. K. W. Li, J.-É. Tremblay, E. C. Carmack, and C. Lovejoy. 2011. Arctic Ocean microbial community structure before and after the 2007 Record Sea ice minimum. PLoS One **6**: e27492. doi:10.1371/journal.pone.0027492

Cruaud, P., A. Vigneron, M. S. Fradette, S. J. Charette, M. J. Rodriguez, C. C. Dorea, and A. I. Culley. 2017. Open the SterivexTM casing: An easy and effective way to improve DNA extraction yields. Limnol. Oceanogr. Methods **15**: 1015–1020. doi:10.1002/lom3.10221

Denfeld, B. A., H. M. Baulch, P. A. del Giorgio, S. E. Hampton, and J. Karlsson. 2018. A synthesis of carbon dioxide and methane dynamics during the ice-covered period of northern lakes. Limnol. Oceanogr. Lett. **3**: 117–131. doi:10.1002/lol2.10079

Frenette, J.-J., P. Thibeault, J.-F. Lapierre, and P. B. Hamilton. 2008. Presence of algae in freshwater ice cover of fluvial Lac Saint-Pierre (St. Lawrence River, Canada). J. Phycol. **44**: 284–291. doi:10.1111/j.1529-8817.2008.00481.x

Grosbois, G., D. Vachon, P. A. del Giorgio, and M. Rautio. 2020. Efficiency of crustacean zooplankton in transferring allochthonous carbon in a boreal lake. Ecology **101**: e03013. doi:10.1002/ecy.3013

Guillemette, F., S. Leigh Mccallister, and P. A. Del Giorgio. 2016. Selective consumption and metabolic allocation of terrestrial and algal carbon determine allochthony in lake bacteria. ISME J. **10**: 1373–1382. doi:10.1038/ismej.2015.215

Hampton, S. E., M. V. Moore, T. Ozersky, E. H. Stanley, C. M. Polashenski, and A. W. E. Galloway. 2015. Heating up a cold subject: Prospects for under-ice plankton research in lakes. J. Plankton Res. **37**: 277–284. doi:10.1093/plankt/fbv002

Hébert, M.-P., B. E. Beisner, M. Rautio, and G. F. Fussmann. 2021. Warming winters in lakes: Later ice onset promotes consumer overwintering and shapes springtime planktonic food webs. Proc. Natl. Acad. Sci. **118**: e2114840118. doi:10.1073/pnas.2114840118

Herlemann, D. P., M. Labrenz, K. Jürgens, S. Bertilsson, J. J. Waniek, and A. F. Andersson. 2011. Transitions in bacterial communities along the 2000 km salinity gradient of the Baltic Sea. ISME J. **5**: 1571–1579. doi:10.1038/ismej.2011.41

Horňák, K., V. Kasalický, K. Šimek, and H. P. Grossart. 2017. Strain-specific consumption and transformation of alga-derived dissolved organic matter by members of the Limnohabitans-C and Polynucleobacter-B clusters of Betaproteobacteria. Environ. Microbiol. **19**: 4519–4535. doi:10.1111/1462-2920.13900

Hrycik, A. R., S. McFarland, A. Morales-Williams, and J. D. Stockwell. 2022. Winter severity shapes spring plankton succession in a small, eutrophic lake. Hydrobiologia **849**: 2127–2144. doi:10.1007/s10750-022-04854-4

Imbeau, E., W. F. Vincent, M. Wauthy, M. Cusson, and M. Rautio. 2021. Hidden stores of organic matter in northern lake ice: Selective retention of terrestrial particles, phytoplankton and labile carbon. J. Geophys. Res. Biogeosci. **126**: e2020JG006233. doi:10.1029/2020JG006233

Ivanova, A. A., I. S. Kulichevskaya, and S. N. Dedysh. 2021. *Gemmata palustris* sp. nov., a novel planctomycete from a fen in northwestern Russia. Microbiol. Russ. Fed. **90**: 598–606. doi:10.1134/S0026261721050076

Jansen, J., and others. 2021. Winter limnology: How do hydrodynamics and biogeochemistry shape ecosystems under ice? J. Geophys. Res. Biogeo. **126**: 1–29. doi:10.1029/2020JG006237

Kankaala, P., J. Huotari, E. Peltomaa, T. Saloranta, and A. Ojala. 2006. Methanotrophic activity in relation to methane efflux and total heterotrophic bacterial production in a stratified, humic, boreal lake. Limnol. Oceanogr. **51**: 1195–1204. doi:10.4319/lo.2006.51.2.1195

Karlsson, J., R. Giesler, J. Persson, and E. Lundin. 2013. High emission of carbon dioxide and methane during ice thaw in high latitude lakes. Geophys. Res. Lett. **40**: 1123–1127. doi:10.1002/grl.50152

Kritzberg, E., and E. Bååth. 2022. Seasonal variation in temperature sensitivity of bacterial growth in a temperate soil and lake. FEMS Microbiol. Ecol. **98**: fiac111. doi:10.1093/femsec/fiac111

Kulichevskaya, I. S., and others. 2020. *Frigoriglobus tundricola* gen. nov., sp. nov., a psychrotolerant cellulolytic planctomycete of the family Gemmataceae from a littoral tundra wetland. Syst. Appl. Microbiol. **43**: 126129. doi:10.1016/j.syapm.2020.126129

Leu, E., C. J. Mundy, P. Assmy, K. Campbell, T. M. Gabrielsen, M. Gosselin, T. Juul-Pedersen, and R. Gradinger. 2015. Arctic spring awakening—Steering principles behind the phenology of vernal ice algal blooms. Prog. Oceanogr. **139**: 151–170. doi:10.1016/j.pocean.2015.07.012

Martinez Arbizu, P. 2020. pairwiseAdonis: Pairwise multilevel comparison using adonis. Available from https://github.com/pmartinezarbizu/pairwiseAdonis

Mazoyer, F., I. Laurion, and M. Rautio. 2022. The dominant role of sunlight in degrading winter dissolved organic matter from a thermokarst lake in a subarctic peatland. Biogeosciences **19**: 3959–3977. doi:10.5194/bg-19-3959-2022

McMeans, B. C., and others. 2020. Winter in water: Differential responses and the maintenance of biodiversity I. Donohue [ed.]. Ecol. Lett. **23**: 922–938. doi:10.1111/ele.13504

McMurdie, P. J., and S. Holmes. 2013. phyloseq: An R package for reproducible interactive analysis and graphics of microbiome census data. PLoS One **8**: e61217. doi:10.1371/journal.pone.0061217

Nusch, E. 1980. Comparison of different methods for chlorophyll and phaeopigment determination. Arch. Hydrobiol. **14**: 14–36.

Obolkin, V. A., E. A. Volkova, S. I. Ohira, K. Toda, O. G. Netsvetaeva, N. S. Chebunina, V. V. Nosova, and N. A. Bondarenko. 2019. The role of atmospheric precipitation in the under-ice blooming of endemic dinoflagellate *Gymnodinium baicalense* var. minor Antipova in Lake Baikal. Limnol. Freshw. Biol. **345–352**: 345–352. doi:10.31951/2658-3518-2019-A-6-345

Oksanen, J., and others. 2020. vegan: Community ecology package. Available from: https://CRAN.R-project.org/package=vegan

Olsthoorn, J., E. W. Tedford, and G. A. Lawrence. 2022. Salt-fingering in seasonally ice-covered lakes. Geophys. Res. Lett. **49**: e2022GL097935. doi:10.1029/2022GL097935

Platt, T., C. L. Gallegos, and W. G. Harrison. 1980. Photoinhibition of photosynthesis in natural assemblages of marine phytoplankton. J. Mar. Res. **38**: 687–701.

Quast, C., E. Pruesse, P. Yilmaz, J. Gerken, T. Schweer, P. Yarza, J. Peplies, and F. O. Glöckner. 2013. The SILVA ribosomal RNA gene database project: Improved data processing and web-based tools. Nucleic Acids Res. **41**: 590–596. doi:10.1093/nar/gks1219

R Core Team. 2023. R: A language and environment for statistical computing. R Foundation for Statistical Computing.

Rae, R., and W. F. Vincent. 1998. Phytoplankton production in subarctic lake and river ecosystems: Development of a photosynthesis-temperature-irradiance model. J. Plankton Res. **20**: 1293–1312. doi:10.1093/plankt/20.7.1293

Reinl, K. L., and others. 2023. Blooms also like it cold. Limnol. Oceanogr. Lett. **lol2.10316**: 546–564. doi:10.1002/lol2.10316

Rott, E., M. Cantonati, L. Füreder, and P. Pfister. 2006. Benthic algae in high altitude streams of the alps—A neglected component of the aquatic biota. Hydrobiologia **562**: 195–216. doi:10.1007/s10750-005-1811-z

Sadro, S., J. O. Sickman, J. M. Melack, and K. Skeen. 2018. Effects of climate variability on snowmelt and implications for organic matter in a high-elevation lake. Water Resour. Res. **54**: 4563–4578. doi:10.1029/2017WR022163

Salmi, P., and K. Salonen. 2016. Regular build-up of the spring phytoplankton maximum before ice-break in a boreal lake. Limnol. Oceanogr. **61**: 240–253. doi:10.1002/lno.10214

Sarmento, H., C. Morana, and J. M. Gasol. 2016. Bacterioplankton niche partitioning in the use of phytoplankton-derived dissolved organic carbon: Quantity is more important than quality. ISME J. **10**: 2582–2592. doi:10.1038/ismej.2016.66

Segata, N., J. Izard, L. Waldron, D. Gevers, L. Miropolsky, W. S. Garrett, and C. Huttenhower. 2011. Metagenomic biomarker discovery and explanation. Genome Biol. **12**: R60. doi:10.1186/gb-2011-12-6-r60

Sharma, S., and others. 2021. Loss of ice cover, shifting phenology, and more extreme events in northern hemisphere lakes. J. Geophys. Res. Biogeo. **126**: e2021JG006348. doi:10.1029/2021JG006348

Shchapov, K., P. Wilburn, A. J. Bramburger, G. M. Silsbe, L. Olmanson, C. J. Crawford, E. Litchman, and T. Ozersky. 2021. Taxonomic and functional differences between winter and summer crustacean zooplankton communities in lakes across a trophic gradient. J. Plankton Res. **43**: 732–750. doi:10.1093/plankt/fbab050

Šimek, K., V. Kasalický, J. Jezbera, J. Jezberová, J. Hejzlar, and M. W. Hahn. 2010. Broad habitat range of the phylogenetically narrow R-BT065 cluster, representing a core group of the Betaproteobacterial genus *Limnohabitans*. Appl. Environ. Microbiol. **76**: 631–639. doi:10.1128/AEM.02203-09

Sime-Ngando, T. 2012. Phytoplankton chytridiomycosis: Fungal parasites of phytoplankton and their imprints on the food web dynamics. Front. Microbiol. **3**: 361. doi:10.3389/fmicb.2012.00361

Smith, D. C., and F. Azam. 1992. A simple, economical method for measuring bacterial protein synthesis rates in seawater using 3H-leucine. Mar. Microb. Food Webs **6**: 107–114.

Smith, E. M., and Y. T. Prairie. 2004. Bacterial metabolism and growth efficiency in lakes: The importance of phosphorus availability. Limnol. Oceanogr. **49**: 137–147. doi:10.4319/lo.2004.49.1.0137

Song, S., and others. 2019. Under-ice metabolism in a shallow lake in a cold and arid climate. Freshw. Biol. **64**: 1710–1720. doi:10.1111/fwb.13363

Straškrábová, V., and others. 2005. Primary production and microbial activity in the euphotic zone of Lake Baikal (Southern Basin) during late winter. Glob. Planet. Change **46**: 57–73. doi:10.1016/j.gloplacha.2004.11.006

Tank, S. E., L. F. W. Lesack, and D. J. McQueen. 2009. Elevated pH regulates bacterial carbon cycling in lakes with high photosynthetic activity. Ecology **90**: 1910–1922. doi:10.1890/08-1010.1

Tran, P., A. Ramachandran, O. Khawasik, B. E. Beisner, M. Rautio, Y. Huot, and D. A. Walsh. 2018. Microbial life under ice: Metagenome diversity and *in situ* activity of *Verrucomicrobia* in seasonally ice-covered lakes. Environ. Microbiol. **20**: 2568–2584. doi:10.1111/1462-2920.14283

Tulonen, T., P. Kankaala, A. Ojala, and L. Arvola. 1994. Factors controlling production of phytoplankton and bacteria under ice in a humic, boreal lake. J. Plankton Res. **16**: 1411–1432. doi:10.1093/plankt/16.10.1411

Twiss, M. R., and others. 2012. Diatoms abound in ice-covered Lake Erie: An investigation of offshore winter limnology in Lake Erie over the period 2007 to 2010. J. Gt. Lakes Res. **38**: 18–30. doi:10.1016/j.jglr.2011.12.008

Vachon, D., and P. A. del Giorgio. 2014. Whole-lake $CO_2$ dynamics in response to storm events in two morphologically different lakes. Ecosystems **17**: 1338–1353. doi:10.1007/s10021-014-9799-8

Vähätalo, A. V., K. Salonen, U. Münster, M. Järvinen, and R. G. Wetzel. 2003. Photochemical transformation of allochthonous organic matter provides bioavailable nutrients in a humic lake. Arch. Hydrobiol. **156**: 287–314. doi:10.1127/0003-9136/2003/0156-0287

van Grinsven, S., J. S. Sinninghe Damsté, A. Abdala Asbun, J. C. Engelmann, J. Harrison, and L. Villanueva. 2020. Methane oxidation in anoxic lake water stimulated by nitrate and sulfate addition. Environ. Microbiol. **22**: 766–782. doi:10.1111/1462-2920.14886

Verpoorter, C., T. Kutser, D. A. Seekell, and L. J. Tranvik. 2014. A global inventory of lakes based on high-resolution satellite imagery. Geophys. Res. Lett. **41**: 6396–6402. doi:10.1002/2014GL060641

Vidal, L. O., W. Granéli, C. B. Daniel, L. Heiberg, and F. Roland. 2011. Carbon and phosphorus regulating bacterial metabolism in oligotrophic boreal lakes. J. Plankton Res. **33**: 1747–1756. doi:10.1093/plankt/fbr059

Warkentin, M., H. M. Freese, U. Karsten, and R. Schumann. 2007. New and fast method to quantify respiration rates of bacterial and plankton communities in freshwater ecosystems by using optical oxygen sensor spots. Appl. Environ. Microbiol. **73**: 6722–6729. doi:10.1128/AEM.00405-07

Winkel, M., C. B. Trivedi, R. Mourot, J. A. Bradley, A. Vieth-Hillebrand, and L. G. Benning. 2022. Seasonality of glacial snow and ice microbial communities. Front. Microbiol. **13**: 876848. doi:10.3389/fmicb.2022.876848

Woolway, R. I., B. Denfeld, Z. Tan, J. Jansen, G. A. Weyhenmeyer, and S. La Fuente. 2022. Winter inverse lake stratification under historic and future climate change. Limnol. Oceanogr. Lett. **7**: 302–311. doi:10.1002/lol2.10231

Yilmaz, P., and others. 2014. The SILVA and "all-species living tree project (LTP)" taxonomic frameworks. Nucleic Acids Res. **42**: 643–648. doi:10.1093/nar/gkt1209

Zhang, W., Y. Zhou, E. Jeppesen, L. Wang, H. Tan, and J. Zhang. 2019. Linking heterotrophic bacterioplankton community composition to the optical dynamics of dissolved organic matter in a large eutrophic Chinese lake. Sci. Total Environ. **679**: 136–147. doi:10.1016/j.scitotenv.2019.05.055

## Acknowledgments

The authors thank Jean-Simon Boulianne for valuable help in the field and Crysta Rhainds in the lab, and are grateful to Forêt d'Enseignement et de Recherche Simoncouche (FERS) of UQAC for providing logistical help. Funding was provided by the Natural Sciences and Engineering Research Council of Canada (NSERC), the Canada Research Chair program, and the Canada Foundation for Innovation (CFI). We thank two reviewers and the editors for their constructive comments.

## Conflict of interest statement

The authors declare no conflict of interest.

*Submitted 03 May 2023*
*Revised 07 September 2023*
*Accepted 07 October 2023*

*Associate editor: Michaela Salcher*